Chinese Chemical Letters 33 (2022) 1613–1618

Contents lists available at ScienceDirect

Chinese Chemical Letters

journal homepage: www.elsevier.com/locate/cclet

Dithienylethene metallodendrimers with high photochromic efficiency

Yuxuan Wang[a,c,1,*], Qifeng Zhou[a,1], Xiaoxiao He[b], Ying Zhang[d], Hongwei Tan[d], Jianhua Xu[b], Cuihong Wang[a,**], Wei Wang[a], Xiping Luo[c], Jinquan Chen[b,**], Lin Xu[a,**]

[a] *Shanghai Key Laboratory of Green Chemistry and Chemical Processes, School of Chemistry and Molecular Engineering, East China Normal University, Shanghai 200062, China*
[b] *State Key Laboratory of Precision Spectroscopy, East China Normal University, Shanghai 200241, China*
[c] *Zhejiang Provincial Key Laboratory of Chemical Utilization of Forestry Biomass, Department of Chemistry, Zhejiang A&F University, Hangzhou 311300, China*
[d] *College of Chemistry, Beijing Normal University, Beijing 100050, China*

ARTICLE INFO

Article history:
Received 12 June 2021
Revised 9 September 2021
Accepted 13 September 2021
Available online 20 September 2021

Keywords:
Photochromic compounds
Stimulus response
Dendrimers
Platinum-acetylide complexes
Dithienylethene

ABSTRACT

It has been challenging to achieve multi-photochromic systems without affecting the individual photoswitching properties of the constituent units. Herein, we present the design and synthesis of a new family of platinum-acetylide dendrimers containing up to twenty-one photochromic dithienylethene (DTE) units that exhibit both high photochromic efficiency and individual switching properties. Upon irradiation with ultraviolet (UV) and visible (vis) light, the resultant metallodendrimers display high conversion yield and good fatigue resistance. More interestingly, cyclization-cycloreversion kinetics revealed that the photochromic property of each DTE unit in these metallodendrimers is unaffected by its neighbor and the full ring-closure of up to twenty-one DTE units in one single dendrimer has been achieved.

Photochromic compounds are light-sensitive molecules that can undergo isomerization between at least two forms. During the past few decades, photochromic systems have attracted more and more attentions since their physicochemical properties can be fine-tuned upon being triggered by light or heat [1–10]. In particular, an increasing effort has been recently devoted to the development of multiphotochromic molecules that are comprised of two or more photochromic because of their wide applications ranging from molecular sensors, molecular motors, energy and information storage devices, photoactuators, and artificial muscles [11–13]. However, in a multiphotochromic system, the steric interaction, interchromophore interaction, excitonic and electronic coupling between adjacent photochromic units usually alter the efficiency and process of photochemical switching, thus leading to the partial photochromic. Therefore, the construction of multi-photochromic systems without affecting the individual photoswitching property of the constituent units remains a great challenge in this field.

Dithienylethene (DTE) represents one of the most popular and extensively studied photoswitches due to its high quantum yield, excellent fatigue resistance and high stability of both isomers, which has been blossoming into an exciting field of research during the past few decades [14–27]. Recently, multiphotochromic compounds based on DTE have been reported. Two or more DTE units are connected covalently *via* organic spacers (methylene, ethynylene, diyne, phenylene, or silyl bridge, *etc.*) or organometallic spacers (Pt-acetylide, Ru-acetylide, or Au-acetylide, *etc.*) in these compounds [28–35]. It should be noted that, rapid energy transfer from the ring-open DTE to an adjacent ring-closed one would be favored instead of full photocyclization in the most cases [36]. Although great efforts have been dedicated to resolving this problem over the past few years [37], achieving full photocyclization of all DTE units in a single multiphotochromic system without affecting the individual photoswitching property is still a difficult task.

Based on our and others' previous study on platinum-acetyide chemistry [38–41], we envisioned that employing platinum-acetylide moieties as bridge to construct multiple DTE systems might be one effective method because the ligand-localized triplet states can be populated and they could inhibit the transfer of excited state energy from ring-open DTE to the ring-closed neighbor. Moreover, platinum-acetylide complexes are thermally robust and stable even upon being exposed to air and moisture [42–51], which can be obtained in high yield by a well-established synthetic

* Corresponding author at: Shanghai Key Laboratory of Green Chemistry and Chemical Processes, Department of Chemistry, East China Normal University, Shanghai 200062, China.
** Corresponding authors.
E-mail addresses: 20190050@zafu.edu.cn (Y. Wang), chwang@chem.ecnu.edu.cn (C. Wang), jqchen@lps.ecnu.edu.cn (J. Chen), lxu@chem.ecnu.edu.cn (L. Xu).
[1] These authors contributed equally to this work.

https://doi.org/10.1016/j.cclet.2021.09.048
1001-8417/

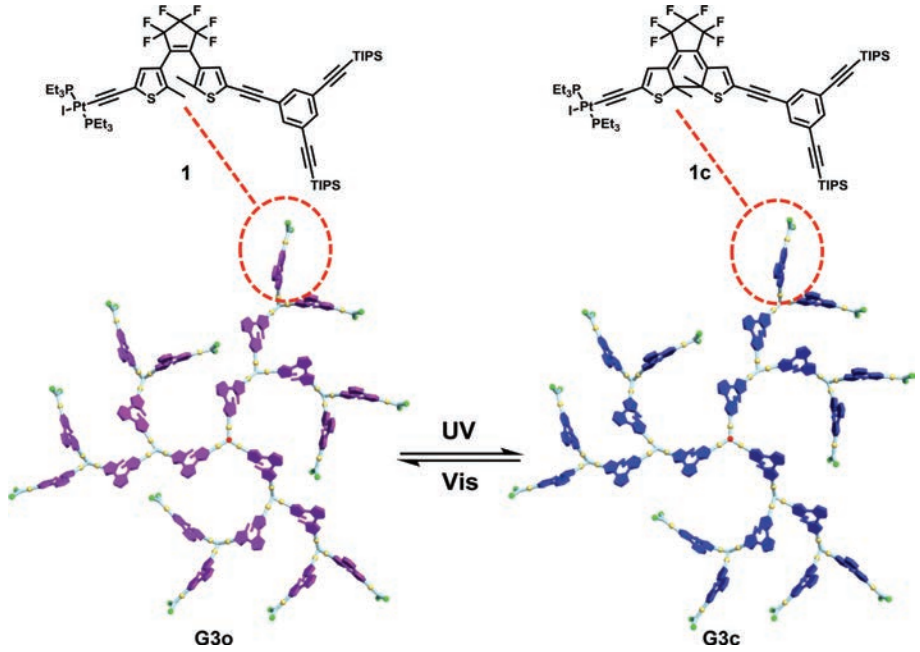

Fig. 1. Schematic representation of the structural transformation of DTE dendrimer. The suffix "o" indicates the ring-open form and "c" indicates the ring-closed form.

methodology. To achieve this goal, dendrimers have evolved to be privileged platforms for the construction of multi-photochromic systems due to their unique highly branched and star-shaped feature [52–56]. Herein, we present an efficient and facile approach for synthesis of multiphotochromic organometallic DTE dendrimers by employing the neutral platinum-acetylides as the main scaffold. More impressively, we have achieved full photocyclization of up to twenty-one DTE units in one single dendrimer (Fig. 1). This approach could be one promising method for designing new multiphotochromic systems without affecting the individual photoswitching property, thus allowing for high photochromic efficiency.

Organometallic complex **1** (Scheme S1 in Supporting information) was employed as the basic precursor for the divergent dendrimer growth for following two reasons: (i) It contains platinum-acetylide unit that can react with alkyne units as well as two protected alkynes that can be gently exposed for dendrimer growth [57–59]; (ii) bis(thien-3-yl) derivatives of perfluorocyclopentene usually exhibit high conversion yields and excellent fatigue-resistant properties. Moreover, the precursor **1** is very stable and soluble in common solvents, which could simplify the subsequent reaction and purification processed during the dendrimer growth [60]. The Cu(I)-catalyzed coupling reaction of **1** with 1,3,5-triethynylbenzene produced the first-generation DTE dendrimer **G1** at yield of 53% (Scheme S3 in Supporting information). By repeating the iterative deprotection–coupling reactions, the construction of the second-generation and third-generation DTE dendrimers **G2** and **G3** (Fig. 2a) were achieved through a divergent approach (Scheme S3 in Supporting information). All obtained dendrimers **Gn** are soluble in common solvents such as chloroform, dichloromethane, and THF. The purification of these dendrimers was performed using flash column chromatography and gel permeation chromatography (GPC).

The structures of the resultant organometallic dendrimers were well characterized by using ^{1}H and ^{31}P NMR spectroscopy (Figs. S4 and S6 in Supporting information and Fig. 2b). **G1** was selected as a representative to illustrate the structural characteristics of resultant DTE dendrimers. The ^{1}H NMR spectrum of **G1** shows five signals at δ 6.74, 6.91, 7.27, 7.51 and 7.54 with an integral ratio of 3:3:3:3:6. The signals at δ 6.74 and 7.27 are assigned to the protons of thiophene heterocycles. The thiophene protons exhibit the upfield shifts resulted from the enhancement of electron density upon covalent linkage with of platinum-acetylide units. The signals at δ 7.51 and 7.54 are assigned to the protons in *para* and *ortho* positions of the outer aromatic rings, respectively. Compared with the organometallic complex **1**, the appearance of the new peak at δ 7.27 attributed to the inner aromatic rings protons indicates the successful coupling of triethynylbenzene with the precursor **1**. Moreover, the ^{31}P NMR spectrum of **G1** shows only one signal at δ 11.5, which is consistent to the phosphorus atoms on triethylphosphine ligands. For **G2**, two sets of signals are observed that are ascribed to different phosphorus atoms of the inner and outer triethylphosphine ligands. ^{31}P NMR spectrum of **G3** also displays two signals because the signals of two outer triethylphosphine ligands could not be well distinguished. Notably, the sharp NMR signals along with the solubility of these species have ruled out the formation of organometallic polymers.

Mass spectrometric studies of the obtained dendrimers **Gn** were performed by using matrix-assisted laser desorption/ionization time of flight mass spectrometry (MALDI-TOF-MS) (Fig. S10 in Supporting information). For **G1**, the MALDI-TOF-MS spectrum in reflection mode exhibits a single peak at *m/z* 3999.1, which is attributed to M^{+} with a theoretical monoisotopic mass at 3994.4. The peak of **G1** is in good agreement with the theoretical distribution. In the case of **G2**, the corresponding peak at *m/z* 10,780.5 is observed in the MS spectrum (theoretical average M = 10,746 Da). The theoretical exact mass of **G3** is 24,249.9 Da that is too large to get a high signal-to-noise ratio peak. Fortunately, the MALDI-TOF-MS spectrum of **G3** shows a single peak at *m/z* 24,396.2, which supports the formation of discrete DTE dendrimer with the third generation.

Two-dimensional diffusion-ordered NMR spectroscopy (2D-DOSY) was performed to obtain the further structural information of the resultant DTE dendrimers in solution (Fig. S9 in Supporting information). A decrease in the measured weight averaged diffusion coefficients (D) (8.13×10^{-9} for **G1**; 6.03×10^{-9} for **G2**; 3.31×10^{-9} for **G3**) is observed, indicating an increase in the hydrodynamic diameter with the growth of dendrimer generation. By studying the direct atomic force microscopy (AFM) images on

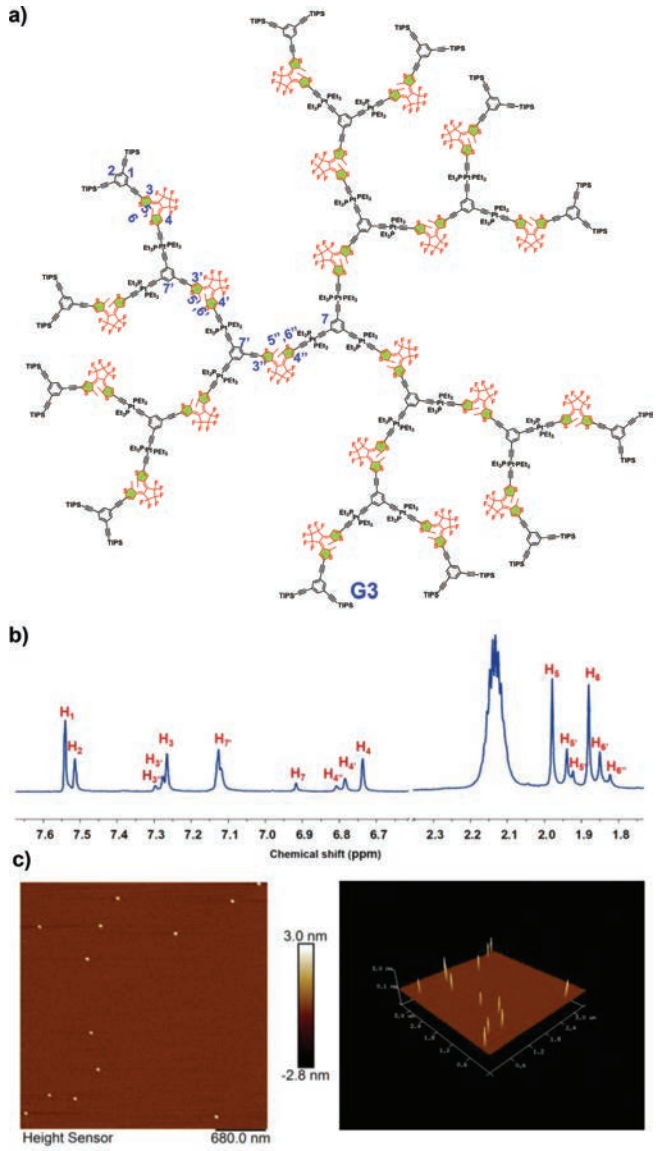

Fig. 2. Characterization of DTE dendrimer **G3**. (a) Structure of **G3**. (b) Partial ^{1}H NMR spectrum (CD_2Cl_2, 500 MHz, r.t.) of **G3**. (c) Two-dimensional (left) and three-dimensional (right) AFM images of **G3**.

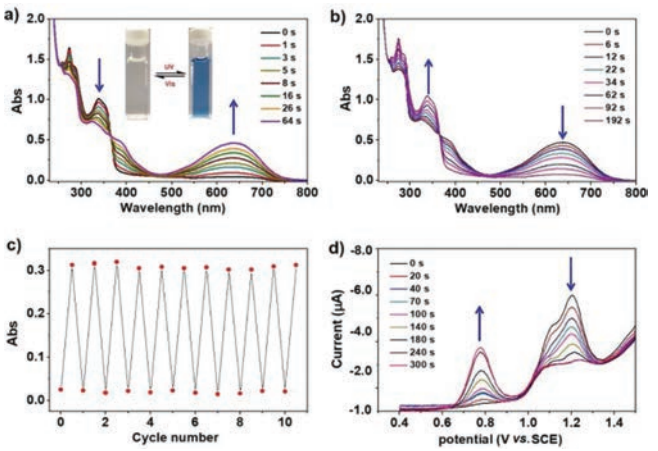

Fig. 3. Characterization of structural transformation of DTE dendrimer **G3**. (a and b) Absorption spectral changes of **G3** (9.5×10^{-8} mol/L in CH_2Cl_2) upon (a) UV (365 nm) irradiation and (b) visible-light (> 530 nm) irradiation. The inset photographic image in (a) shows the color changes of **G3** upon alternating UV and visible-light irradiation. (c) Fatigue resistance of **G3** upon alternating UV (365 nm) and visible-light (> 530 nm) irradiation. (d) Changes in the differential pulse voltammograms of **G1** (2×10^{-5} mol/L in CH_2Cl_2) irradiation at 365 nm. For interpretation of the references to color in this figure legend, the reader is referred to the web version of this article.

a surface, the structural parameters of the DTE dendrimers could be obtained. As shown in Fig. S11 (Supporting information), a consistent set of small particles are observed in AFM images of **Gn**, which are attributed to the adsorbed DTE dendrimers species, respectively. The detailed cross-sectional measurements on a large number of isolated features reveal the gradually increased average heights with each generation of dendrimers (*ca.* 1.0 nm for **G1**; *ca.* 1.9 nm for **G2**; *ca.* 3.1 nm for **G3** (Fig. 2c)).

The light-driven switching of these dendrimers was firstly studied by ^{1}H and ^{31}P NMR spectroscopy. Again, **G1** was selected as a representative to illustrate such light-driving switching process. When the solution of **G1** in CH_2Cl_2 (1.2×10^{-4} mol/L) was irradiated with UV light at 365 nm, the ^{1}H NMR spectral signals at δ 6.78 for H_4 and 7.31 for H_3 are gradually weakened and finally disappeared, where two new signals at δ 6.07 for H_4 and 6.50 for H_3 are increasingly enhanced due to the photocyclization reaction **G1o** → **G1c**. The loss of aromaticity of the thiophene heterocycles in the photocyclization reaction leads to this characteristic upfield. The signals of the -CH_3 proton of **G1o** are observed at δ 2.02 (H_5) and 1.91 (H_6). Upon irradiation of **G1o** under UV light at 365 nm, the two signals are gradually attenuated and finally vanished with the occurrence of two new CH_3 signals at δ 2.19 (H_5) and 2.18 (H_6). The similar results were observed in the case of **G2** and **G3**. It should be noted that, in the more complex case of **G3**, the signals at δ 7.27, 7.28 and 7.30 that are assigned to the protons of three layered thiophene heterocycles shift upfield to the signals at δ 6.46 and 6.45, which are assigned to the ring-closed inner two and outer DTE units with the integral ratio 3:4 ((3 + 6):12). The photochromic reaction **G1o** → **G1c** has been also supported by ^{31}P NMR spectroscopy. When a CH_2Cl_2 solution of **G1o** is irradiated at 365 nm, the phosphorus signal at δ 11.51 decreases gradually and finally vanishes, whereas a new broad phosphorous signal is observed at δ 11.90. It reveals that **G1o** is converted to **G1c** quickly upon irradiation at 365 nm and the single ring-closed intermediate did not appear. At the photostationary state (PSS), the integral ratio of phosphorous signals between **G1o** and **G1c** suggest the presence of *ca.* 95% of **G1c** and 5% of **G1o**. The transformation behavior induced by light irradiation of **Gn** was further investigated by UV–vis techniques (Figs. 3a and b). The absorption spectrum of **G3** (in CH_2Cl_2 at 298 K) exhibits an intense band in the near-UV region (*ca.* 330 nm) with the weaker transition at higher energy (*ca.* 275 nm). Upon irradiation at 365 nm, the colourless solution of **G3** quickly turns to blue (insert in Fig. 3a). Notably, two new absorption bands at 390 and 637 nm are observed in the visible region along with a well-defined isosbestic point at 374 nm arising from the corresponding ring-closed photostationary state (PSS) of **G3** *via* the typical photocyclization. During light irradiation, the UV–vis changes are simple and clean with a well-defined isosbestic point, which provides evidence for the existence of only two light-absorbing components. This means that each photochromic unit is isolated from the others [33,37]. According to the previous study on DTE-based systems, the low energy absorption is attributed to the π-conjugation delocalizing throughout the DTE ligands due to the formation of ring-closed form, then leading to the decrease of HOMO-LUMO gap. Similarly, UV irradiation of **G1** or **G2** at 365 nm in CH_2Cl_2 results in the ring-closed PSS of **G1** or **G2**, respectively, accompanied by a color change from colourless to blue along with the formation of two intense absorption bands at 390 and 637 nm. Moreover, the photoisomerization between the ring-open and ring-

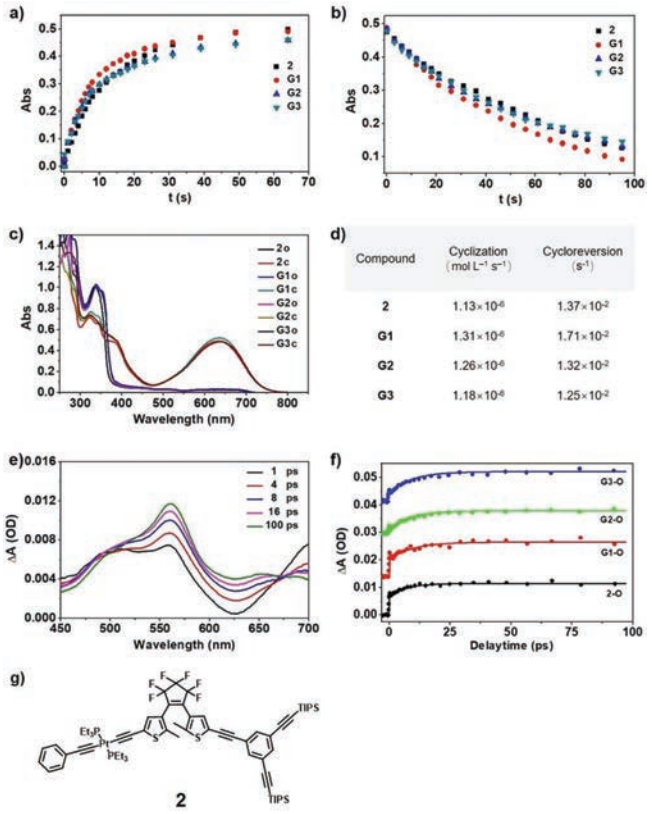

Fig. 4. Cyclization-cycloreversion kinetics studies of organometallic complex **2** and the DTE dendrimers **Gn.** (a and b) Absorption spectral changes at 637 nm of **2** (2.0×10^{-5} mol/L), **G1** (6.7×10^{-6} mol/L), **G2** (2.2×10^{-7} mol/L) and **G3** (9.5×10^{-8} mol/L) upon UV irradiation at 365 nm (a) and visible-light irradiation (> 530 nm) (b). (c) UV–vis absorption spectra of ring-open and ring-closed form of **2** and **Gn**. (d) The rate constants of cyclization and cycloreversion processes of **2** and **Gn**. (e) Femtosecond transient absorption spectra of sample **2** under 365 nm excitation. (f) Kinetics of sample **2**, **G1**, **G2** and **G3** monitored at 560 nm. (g) Structure of model complex **2**.

closed forms of the dithienylethene moieties could be repeated more than ten times (Fig. 3c). The dendrimer **G1** exhibits an irreversible Pt-based oxidation wave at 1.21 V together with an irreversible DTE-centered wave at 1.11 V (Fig. 3d). Upon irradiation of **G1** at 365 nm to the PSS, the oxidation potentials of both Pt- and DTE-centered waves are distinctly less anodic because of the enhanced π-electron density with photocyclization at both DTE units. Particularly, the presence of two successive DTE-based oxidation waves at 0.78 V and 1.05 V for **G1c** suggests that the moderate electron interaction is likely mediated between the ring-closed DTE units across the *trans*-Pt$(PEt_3)_2$ spacer [61].

To better understand the photochromic process of the DTE dendrimers, a model complex **2** was prepared from the precursor **1** (Scheme S2 in Supporting information). The cyclization and cycloreversion kinetics of DTE dendrimers **Gn** and the model **2** were investigated by irradiation by UV (365 nm) or visible light (> 530 nm) (Fig. 4). As shown in Fig. 4a, the cyclization kinetics of **Gn** and **2** show that the photochromic cyclization reaction followed the zeroth-order reaction kinetics; the relationships between absorbance and exposure time (A *vs.* t) display a good linearity upon irradiation with UV light (365 nm). Due to the darker color of the solution that affected the absorption of UV light upon irradiation with UV light, the first nine points are plotted to on the graph. The slopes of the A *vs.* t lines give the zeroth order rate constant, $k_{o\text{-}c}$. According to this method, all the k values for the cyclization process ($k_{o\text{-}c}$) of the dendrimers **Gn** and the complex **2** are readily determined to be 1.13×10^{-6}, 1.31×10^{-6}, 1.26×10^{-6}, and 1.18×10^{-6} mol L^{-1} s^{-1}, respectively. Similarly, the cycloreversion kinetic curves shown in Fig. 4b indicate that the photochromic cyclization reaction followed first-order reaction kinetics. The rate constant k of the cycloreversion process of DTE dendrimers **Gn** and the complex **2** are calculated to be 1.71×10^{-2}, 1.32×10^{-2}, 1.25×10^{-2}, and 1.37×10^{-2} s^{-1}, respectively. Importantly, the rates of photochromic process for the DTE dendrimers and the complex **2** are essentially identical, indicating that each switching units behaved independently (Fig. 4d). Upon irradiation at 365 nm, both the DTE dendrimers **Gn** and the model organometallic complex **2** undergo photocyclization with the similar maximum at 637 nm. The molar absorptivity of **G1**–**G3** is 3, 9 or 21 times that of **2**, confirming that the PSS (in terms of the total number of photochromic units) for **Gn** is essentially identical to **2**.

The dynamics of cyclization of diarylethene derivatives were previous studied by time-resolved spectroscopy [62–65] and the ring-close reaction was found to take place within several ps. Therefore, we further investigated mechanism of the cyclization reaction for model complex **2** and DTE dendrimers **Gn** by using femtosecond transient absorption (TA) spectroscopy. As shown in Fig. 4e the upper panel, complex **2** shows one broad excited state absorption (ESA) band (450–600 nm) with two peaks at 500 and 560 nm as well as a second ESA band (620–750 nm) with its maximum at 700 nm immediately after photo excitation. In the next 100 ps, the intensity of the 560 nm ESA signal gradually increases while the intensity of the red side ESA band decreases. Finally, a new ESA peak centered at 650 nm shows up and this peak matches well with the steady-state absorption of complex **2** (Fig. 4c) in the ring-closed form, indicating the finish of ring-close reaction in this compound. After 100 ps (Fig. 4e the lower panel), there is bare any spectra evolution and the whole ESA signal decay together in our 7.0 ns detection time window. The initial build-up of the ESA signal were used to analyze the time profiles of the ring-close reaction in previous time-resolved studies [63–65] and we chose the kinetic trace at 560 nm to reveal the time scale of ring closure for complex **2** in this study. The best-fit (τ_2, Table S1 in Supporting information) shows that the build-up lifetime for complex **2** is 7.4 ± 0.8 ps and this value is in line with those determined for diarylethene derivatives in literatures [62–64]. Thus, we conclude that the ring closure reaction of our model complex **2** should finish in ~7.0 ps after photo excitation.

TA experiments were also carried out on DTE dendrimers **Gn** under the same condition and the spectra are shown in Fig. S15 (Supporting information). Very similar time-resolved spectra behavior was observed for sample **G1–G3**, suggesting these samples could have the same cyclization reaction mechanism. Kinetic traces at 560 nm (Fig. 4f) clearly demonstrate that sample **G1–G3** should have almost the identical signal build-up process. The best fit lifetimes (Table S1) are determined to be 9.9 ± 1.5 ps, 10.8 ± 0.8 ps and 11.4 ± 1.1 ps for **G1–G3**, respectively, and these values agree with each other within experimental uncertainty. Since the total number of photochromic units in sample **G1–G3** is also the same in our TA experiments, the almost identical ESA build-up lifetimes and TA signal intensities are the direct evidence to show that the ring closure time is ~10 ps no matter there are 3, 9 or 21 DTE units in our DTE dendrimers.

TD-DFT calculations were performed on **G1** to learn more about the independent switching units. The simulated absorption spectra of the four structures obtained upon successive DTE cyclisations are given in Fig. 5, whereas Fig. 5a lists the corresponding and the relative total energies. The relative energies regularly increase by 7.96 kcal/mol for each electrocyclization, a typical cost of unconstrained DTE unit. Indeed, a strong UV band corresponding to the lowest energetic transition of each isolated ring-closed DTE unit is

a)

Isomer	ΔE (kcal/mol)	λ_{abs} (UV)	λ_{abs} (Vis)
3o	0.00	366.19 (2.06)	
2o1c	-7.96	362.33 (1.91)	644.67 (0.58)
1o2c	-15.87	384.76 (0.70)	650.78 (1.37)
3c	-23.70	384.05 (0.37)	649.37 (2.73)

b)

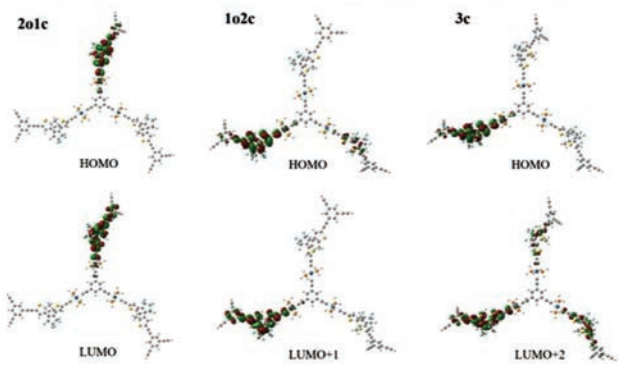

Fig. 5. Computational studies of **G1**. (a) Relative energies (ΔE (kcal/mol)) and main visible absorption bands (obtained after convolution) for the different isomers of **G1**. (b) Molecular orbitals of three isomers of **G1**. The suffix "o" indicates the ring-open form and "c" indicates the ring-closed form. **3o, 2o1c, 1o2c** and **3c** are **G1** isomers with three ring-open form, two ring-open form, one ring-open form and three ring-closed form DTE units.

found in **G1** (**3o**), whereas in **G1** (**1c2o**), the intensity of this band decreases while a new band corresponding to the second energetic transition of ring-closed form DTE at the longer wavelengths appears. The nature of the molecular orbital transitions assigned to the main visible spectra in the different isomers was investigated. The energy gap of the molecular orbital transitions between HOMO and LUMO of **G1** (**2c1o**) corresponding to the absorption band at *ca.* 645 nm is 2.4 eV, which is same as the energy gap of **G1** (**1c2o**) and **G1** (**3o**). Besides, as shown in the simulated molecular model of **G1**, the benzene core could prevent the effective energy transfer between the photochromes due to the twists between the phenyl ring and platinum-acetylide units (Fig. 5b). All these observations are consistent with the experimental trends and hint that the three DTE could be viewed as independent photochromic entities rather than a conjugated ensemble.

In summary, a new family of miltiple DTE metallodendrimers was prepared by using platinum-acetylide moieties as bridges. UV–vis absorption spectra and multinuclear NMR spectroscopy suggested the high transformation rate, high conversion yield and excellent fatigue resistance of the resultant DTE dendrimers. Cyclization-cycloreversion kinetics studies demonstrate that twenty-one DTE units are rather independent, *i.e.*, the electronic feature of a DTE being is unaffected by the nature of its neighbors. This approach to arranging chromophores is expected to be general and allow for straightforward synthetic access to systems, in which multiple photochemical and redox-active units are arranged with a high degree of order and retention of molecular properties, thus allowing for their promising applications in various photonic devices such as optical memory and organic light-emitting diodes in the future.

Declaration of competing interest

The authors declare that they have no known competing financial interests or personal relationships that could have appeared to influence the work reported in this paper.

Acknowledgments

This work was supported by the National Natural Science Foundation of China (Nos. 11674101, 21873030, 91850202, and 21871092), and the Fundamental Research Funds for the Central Universities.

Supplementary materials

Supplementary material associated with this article can be found, in the online version, at doi:10.1016/j.cclet.2021.09.048.

References

[1] W. Szymański, J.M. Beierle, H.A.V. Kistemaker, W.A. Velema, B.L. Feringa, Chem. Rev. 113 (2013) 6114–6178.
[2] H.K. Bisoyi, Q. Li, Chem. Rev. 116 (2016) 15089–15166.
[3] R. Pardo, M. Zayat, D. Levy, Chem. Soc. Rev. 40 (2011) 672–687.
[4] S. Kawata, Y. Kawata, Chem. Rev. 100 (2000) 1777–1788.
[5] Y. Liu, Q. Peng, Y. Li, H. Hou, K. Li, Chin. Chem. Lett. 31 (2020) 3271–3275.
[6] Y. Pan, C. Zhang, S.H. Liu, Y. Tan, J. Yin, Dyes Pigm. 181 (2020) 108546.
[7] L. Ma, C. Li, Q. Yan, et al., Chin. Chem. Lett. 31 (2020) 361–364.
[8] Z. Li, Y. Wang, M. Li, et al., Org. Biomol. Chem. 16 (2018) 6988–6997.
[9] Y. Wu, Z. Guo, W.H. Zhu, et al., Mater. Horiz. 3 (2016) 124–129.
[10] Y. Cai, Z. Guo, J. Chen, et al., J. Am. Chem. Soc. 138 (2016) 2219–2224.
[11] A. Perrier, F. Maurel, D. Jacquemin, Acc. Chem. Res. 45 (2012) 1173–1182.
[12] A. Fihey, A. Perrier, W.R. Browne, D. Jacquemin, Chem. Soc. Rev. 44 (2015) 3719–3759.
[13] M. Li, S. Yang, W. Liang, X. Zhang, D. Qu, Dyes Pigm. 166 (2019) 239–244.
[14] M. Irie, Chem. Rev. 100 (2000) 1685–1716.
[15] M. Irie, T. Fukaminato, K. Matsuda, S. Kobatake, Chem. Rev. 114 (2014) 12174–12277.
[16] H. Tian, S. Yang, Chem. Soc. Rev. 33 (2004) 85–97.
[17] Y. Cai, Z. Guo, J. Chen, et al., J. Am. Chem. Soc. 138 (2016) 2219–2224.
[18] H. Yang, M. Li, C. Li, et al., Angew. Chem. Int. Ed. 59 (2020) 8560–8570.
[19] Y. Gu, E.A. Alt, H. Wang, et al., Nature 560 (2018) 65–69.
[20] Y.X. Wang, Q.F. Zhou, S.T. Jiang, et al., Macromol. Rapid Commun. 39 (2018) 1800454.
[21] Y. Qin, Y. Zhang, G.Q. Yin, et al., Chin. J. Chem. 37 (2019) 323–329.
[22] R. Li, J.J. Holstein, W.G. Hiller, J. Andréasson, G.H. Clever, J. Am. Chem. Soc. 141 (2019) 2097–2103.
[24] R. Li, J. Tessarolo, H. Lee, G.H. Clever, J. Am. Chem. Soc. 143 (2021) 3865–3873.
[25] Q. Ling, T. Cheng, S. Tan, J. Huang, L. Xu, Chin. Chem. Lett. 31 (2020) 2884–2890.
[26] Y. Qin, L.J. Chen, Y. Zhang, et al., Chem. Commun. 55 (2019) 11119–11122.
[27] J. Zhu, X. Liu, J. Huang, L. Xu, Chin. Chem. Lett. 30 (2019) 1767–1774.
[28] A. Peter, N.R. Branda, Adv. Mater. Opt. Electron. 10 (2000) 245–249.
[29] T. Kaieda, S. Kobatake, H. Miyasaka, et al., J. Am. Chem. Soc. 124 (2002) 2015–2024.
[30] K. Yagi, M. Irie, Chem. Lett. 32 (2003) 848–849.
[31] K. Matsuda, M. Irie, J. Am. Chem. Soc. 123 (2001) 9896–9897.
[32] J. Areephong, W.R. Browne, B.L. Feringa, Org. Biomol. Chem. 5 (2007) 1170–1174.
[33] M.N. Roberts, C. Carling, J.K. Nagle, N.R. Branda, M.O. Wolf, J. Am. Chem. Soc. 131 (2009) 16644–16645.
[34] B. Li, H. Wen, J. Wang, L. Shi, Z. Chen, Inorg. Chem. 52 (2013) 12511–12520.
[35] B. Li, J. Wang, H. Wen, L. Shi, Z. Chen, J. Am. Chem. Soc. 134 (2012) 16059–16067.
[36] D. Jacquemin, E.A. Perpète, F. Maurel, A. Perrier, Phys. Chem. Chem. Phys. 12 (2010) 7994–8000.
[37] J. Areephong, H. Logtenberg, W.R. Browne, B.L. Feringa, Org. Lett. 12 (2010) 2132–2135.
[38] W. Wang, H.B. Yang, Chem. Commun. 50 (2014) 5171–5186.
[39] L. Xu, H.B. Yang, Chem. Rec. 16 (2016) 1274–1297.
[40] W.J. Li, Z. Hu, L. Xu, et al., J. Am. Chem. Soc. 142 (2020) 16748–16756.
[41] J.L. Zhu, L. Xu, Y.Y. Ren, et al., Nat. Commun. 10 (2019) 4285.
[42] A.Y.Y. Tam, V.W.W. Yam, Chem. Soc. Rev. 43 (2013) 1540–1567.
[43] C. Po, V.W.W. Yam, Chem. Sci. 5 (2014) 4868–4872.
[44] K. Chan, C.Y.S. Chung, V.W.W. Yam, Chem. Eur. J. 21 (2015) 16434–16447.
[45] G.J. Zhou, W.Y. Wong, Chem. Soc. Rev. 40 (2011) 2541–2566.
[46] C.L. Ho, Z.Q. Yu, W.Y. Wong, Chem. Soc. Rev. 5 (2016) 5264–5295.
[47] T. Cardolaccia, Y. Li, K.S. Schanze, J. Am. Chem. Soc. 130 (2008) 2535–2545.
[48] Y. Han, Y. Tian, Z. Li, F. Wang, Chem. Soc. Rev. 47 (2018) 5165–5176.
[49] M. Liu, Y. Han, H. Zhong, X. Zhang, F. Wang, Angew. Chem. Int. Ed. 60 (2021) 3498–3503.
[50] Y. Furusho, Y. Tanaka, E. Yashima, Org. Lett. 8 (2006) 2583–2586.
[51] H. Ito, M. Ikeda, T. Hasegawa, Y. Furusho, E. Yashima, et al., J. Am. Chem. Soc. 133 (2011) 3419–3432.
[52] G.R. Newkome, C.N. Moorefield, Chem. Soc. Rev. 44 (2015) 3954–3967.
[53] H. Sun, S. Zhang, V. Percec, Chem. Soc. Rev. 44 (2015) 3900–3923.
[54] W. Qiao, P. Zhang, L. Sun, et al., Chin. Chem. Lett. 31 (2020) 2742–2746.
[55] W.J. Li, X.Q. Wang, D.Y. Zhang, et al., Angew. Chem. Int. Ed. 60 (2021) 18761–18768.
[56] W.J. Fan, B. Sun, J. Ma, et al., Chem. Eur. J. 21 (2015) 12947–12959.
[57] W. Wang, L.J. Chen, X.Q. Wang, et al., Proc. Natl. Acad. Sci. U. S. A. 112 (2015) 5597–5601.
[58] X.Q. Wang, W. Wang, W.J. Li, et al., Nat. Commun. 9 (2018) 3190.
[59] Y.X. Wang, Q.F. Zhou, L.J. Chen, et al., Chem. Commun. 54 (2018) 2224–2227.

[60] K. Albrecht, Y. Hirabayashi, M. Otake, et al., Sci. Adv. 2 (2016) e1601414.
[61] T. Yang, S. Pu, B. Chen, J. Xu, Can. J. Chem. 85 (2007) 12–20.
[62] H. Miyasaka, T. Nobuto, M. Murakami, et al., J. Phys. Chem. A 106 (2002) 8096–8192.
[63] P.R. Hania, A. Pugzlys, L.N. Lucas, et al., J. Phys. Chem. A 109 (2005) 9437–9442.
[64] K. Tani, Y. Ishibashi, H. Miyasaka, S. Kobatake, M. Irie, J. Phys. Chem. C 112 (2008) 11150–11157.
[65] Y. Ishibashi, M. Fujiwara, T. Umesato, et al., J. Phys. Chem. C 115 (2011) 4265–4272.